

**T.C.  
ISTANBUL AYDIN UNIVERSITY  
INSTITUTE OF GRADUATE STUDIES**



**ANALYSIS OF 400-KW GRID-CONNECTED PV FARM UNDER  
DIFFERENT LOAD CONDITION**

**MASTER'S THESIS**

**Samin SARRAF BOSHROUEI**

**Department of Electrical and Electronics Engineering  
Electrical and Electronics Engineering Program**

**JULY, 2023**



**T.C.  
ISTANBUL AYDIN UNIVERSITY  
INSTITUTE OF GRADUATE STUDIES**



**ANALYSIS OF 400-KW GRID-CONNECTED PV FARM UNDER  
DIFFERENT LOAD CONDITION**

**MASTER'S THESIS**

**Samin SARRAF BOSHROUEI**

**(Y2113.300009)**

**Department of Electrical and Electronics Engineering  
Electrical and Electronics Engineering Program**

**Thesis Advisor: Prof. Dr. Murteza FARSADI**

**JULY, 2023**

## ONAY FORMU

## **DECLARATION**

I hereby declare with the respect that the study “Analysis of 400-kW Grid-Connected PV Farm Under Different Load Condition”, which I submitted as a Master thesis, is written without any assistance in violation of scientific ethics and traditions in all the processes from the project phase to the conclusion of the thesis and that the works I have benefited are from those shown in the References. (16/08/2023)

Samin SARRAF BOSHROUEI

## **PREFACE**

I would like to express my gratitude to my advisor, Dr. Farsadi, for his support and encouragement during my Master's studies at Istanbul Aydin University. I am thankful for the experiences and opportunities he provided for me to grow individually and professionally.

I am very grateful to my parents and my uncle for their unlimited support and motivation.

Finally, I would like to acknowledge the important contribution of Istanbul Aydin University to my professional life.

July, 2023

Samin SARRAF BOSHROUEI

# **ANALYSIS OF 400-KW GRID-CONNECTED PV FARM UNDER DIFFERENT LOAD CONDITION**

## **ABSTRACT**

Population growth is driving up power demand; this, in principle, can give rise to energy production and distribution. Clean, green, and sustainable energy sources have drawn attention as the world has advanced. SDG 7 (Sustainable Development Goals) from “Transforming our world: the 2030 Agenda for Sustainable Development” assures that by the end of 2030, everyone will have access to modern, sustainable, reliable, and affordable energy.

This study aims to simulate and analyze a 400 kW grid-connected photovoltaic (PV) system. Specifically, we aim to find a valid performance range for the presented system. The system is made up of four PV arrays with a capacity of 100 kW. The PV arrays are connected to DC/DC boost converter where the individual maximum power point trackers (MPPT) are located. Using MPPT enables the system to extract the PV array’s maximum productivity. To find the maximum power point, Perturb and Observe (P&O) technique was used. A three-phase voltage source converter (VSC) is used in the simulated system to convert 500 V DC to 260 V AC while keeping a unity power factor. In addition, a three-phase coupling transformer with a capacity of 400 kVA 260 V/25 kV is designed to connect the converter to the power grid. The simulated utility grid is a typical North American grid, including a 25 kV distribution feeder and 120 kV equivalent transmission system. Both active and reactive loads were investigated in this study. The system was tested under different load conditions, such as series and parallel RLC loads with different load profiles.

**Keywords:** Performance Analysis, Grid-connected PV system, SDG7, Renewable Energy, MATLAB/Simulink Simulation

## 400-KW ŞEBEKE BAĞLANTILI PV ENERJİ SANTRALİN FARKLI YÜK KOŞULLARI ALTINDA ANALİZİ

### ÖZET

Nüfus artışı enerji talebini yükseltmektedir; bu durum prensip olarak enerjinin üretim ve dağıtımını artırabilir. Dünya ilerleme kaydettikçe temiz, yeşil ve sürdürülebilir enerji kaynakları dikkat çekmeye başlamıştır. "Dünyamızı Dönüştürmek: Sürdürülebilir Kalkınma için 2030 Gündemi"nden SDG 7 (Sürdürülebilir Kalkınma Hedefi), 2030'un sonuna kadar herkesin modern, sürdürülebilir, güvenilir ve uygun fiyatlı enerjiye erişebileceğini güvenceye almaya amaçlar.

Bu çalışma, 400 kW'lık şebeke bağlantılı bir fotovoltaik (PV) sistemi simüle ve analiz etmeyi hedeflemektedir. Spesifik olarak, sunulan sistem için geçerli bir performans aralığı bulmaya amaçlanmıştır. Sistem, 100 kW kapasiteli dört adet PV dizisinden oluşmaktadır. PV dizileri, bireysel maksimum güç noktası izleyicilerinin (MPPT) bulunduğu DC/DC yükseltici dönüştürücüye bağlanır. MPPT'nin kullanılması, sistemin PV dizisinin maksimum üretkenliğini çıkarmasını sağlar. Maksimum güç noktasını bulmak için Perturb and Observe (P&O) tekniği kullanılmıştır. Simüle edilmiş sistemde, birlik güç faktörü altında 500 V DC'yi 260 V AC'ye dönüştürmek için üç fazlı bir gerilim kaynağı dönüştürücü (VSC) kullanılmıştır. Ayrıca, dönüştürücüyü elektrik şebekesine bağlamak için 400 kVA 260 V/25 kV kapasiteli üç fazlı bir kuplaj transformatörü tasarlanmıştır. Simüle edilmiş elektrik şebekesi, 25 kV dağıtım besleyici (feeder) ve 120 kV eşdeğer iletim sistemi içeren tipik bir Kuzey Amerika şebekesidir. Bu çalışmada hem aktif hem de reaktif yükler incelenmiştir. Sistem, farklı yük profillerine sahip seri ve paralel RLC yükleri gibi farklı yük koşullarında test edilmiştir.

**Anahtar Kelimeler:** Performans Analizi, Şebeke Bağlantılı PV Sistemi, SDG7, Yenilenebilir Enerji, MATLAB/Simulink Simülasyonu

## TABLE OF CONTENTS

<b>DECLARATION</b> .....	<b>i</b>
<b>PREFACE</b> .....	<b>ii</b>
<b>ABSTRACT</b> .....	<b>iii</b>
<b>ÖZET</b> .....	<b>iv</b>
<b>TABLE OF CONTENTS</b> .....	<b>v</b>
<b>ABBREVIATIONS</b> .....	<b>vii</b>
<b>LIST OF TABLES</b> .....	<b>ix</b>
<b>LIST OF FIGURES</b> .....	<b>x</b>
<b>I. INTRODUCTION</b> .....	<b>1</b>
A. Background .....	1
B. Problem Statement.....	3
C. Objective of the Research .....	3
D. Research Methodology .....	4
E. Scope of the Thesis .....	5
F. Significance of the Research .....	5
<b>II. LITERATURE REVIEW</b> .....	<b>6</b>
A. Introduction .....	6
B. PV System Classification .....	8
1. Grid-Connected PV System .....	9
1.1. Components a of Grid-Connected PV System .....	9
1.2. Design of a Grid-Connected PV System.....	10
2. Stand-Alone PV System.....	10
2.1. Components of a Stand-Alone PV System .....	11
2.2. Design of a Stand-Alone PV System .....	11
3. Hybrid PV System .....	12
C. Grid Integration of Solar PV Systems .....	12
<b>III. MODELING OF GRID-CONNECTED PV SYSTEM</b> .....	<b>14</b>

A. Introduction .....	14
B. System Overview .....	14
C. Modeling of System Components .....	15
1. PV Array .....	15
2. DC/DC Boost Converter .....	16
2.1. Control Strategy .....	16
3. Voltage Source Converter .....	18
4. Capacitor Bank.....	19
5. Coupling Transformer.....	20
6. RLC Load Block .....	20
7. Utility Grid.....	21
<b>IV. SIMULATION RESULTS AND DISCUSSION.....</b>	<b>22</b>
A. Introduction .....	22
B. System Simulation.....	22
C. Performance Analysis.....	34
1. Performance Analysis Under Active Loads.....	34
2. Performance Analysis Under Active and Reactive Loads .....	35
2.1. Series RLC Load .....	35
2.2. Parallel RLC Load.....	37
<b>V. CONCLUSION AND FUTURE WORKS .....</b>	<b>40</b>
<b>VI. REFERENCES.....</b>	<b>42</b>

## **ABBREVIATIONS**

<b>AC</b>	: Alternating Current
<b>Al-BSF</b>	: Aluminum Back Surface Field
<b>ANN</b>	: Artificial Neural Network
<b>BSF</b>	: Back Surface Field
<b>CUF</b>	: Capacity Utilization Factor
<b>DC</b>	: Direct Current
<b>DR</b>	: Distributed Resources
<b>HIT</b>	: Heterojunction with an intrinsic thin layer
<b>HJT</b>	: Hetero-Junction
<b>HOMER</b>	: Hybrid Optimization of Multiple Energy Resources
<b>HT</b>	: High Tension
<b>I</b>	: Current
<b>IBC</b>	: Inter Digitated Back Contact
<b>IEA</b>	: International Energy Agency
<b>IEC</b>	: International Electrotechnical Commission
<b>Imp</b>	: Current at maximum power point
<b>Ir</b>	: Irradiance
<b>Isc</b>	: Short-circuit Current
<b>LOLP</b>	: Loss Of Load Probability
<b>LT</b>	: Low Tension
<b>MPPT</b>	: Maximum Power Point Tracker

<b>P</b>	: Active Power
<b>P&amp;O</b>	: Perturb and Observe
<b>PCU</b>	: Power Conditioning Unit
<b>PERC</b>	: Passivation Emitter and Rear Contact
<b>PERL</b>	: Passive Emitter Rear Locally diffused
<b>PERT</b>	: Passive Emitter Rear Totally diffused
<b>PFA</b>	: Performance Forecasting Approach
<b>PLF</b>	: Plant Load Factor
<b>Pm</b>	: Mean Power
<b>PPA</b>	: Power Purchase Agreement
<b>PV</b>	: Photovoltaic
<b>PV1</b>	: First Photovoltaic Array
<b>PV2</b>	: Second Photovoltaic Array
<b>PV3</b>	: Third Photovoltaic Array
<b>PV4</b>	: Forth Photovoltaic Array
<b>PWM</b>	: Pulse Width Modulation
<b>Q</b>	: Reactive Power
<b>RE</b>	: Renewable Energy
<b>RES</b>	: Renewable Energy Sources
<b>RLC</b>	: Resistor Inductor Capacitor
<b>SCADA</b>	: Supervisory Control And Data Acquisition
<b>SDG</b>	: Sustainable Development Goals
<b>V</b>	: Voltage
<b>Vmp</b>	: Voltage at maximum power point
<b>Voc</b>	: Open circuit voltage
<b>VSC</b>	: Voltage Source Converter

## LIST OF TABLES

Table 1 Technical Specifications of SunPower SPR-315E module.....	15
Table 2 Model parameters for SunPower SPR-315E.....	15
Table 3 PV array's matrix for time and amplitude of the irradiance .....	22
Table 4 Measured parameters for PV arrays with respect to the given temperature in robust discrete model .....	23
Table 5 PV1 measured parameters in MATLAB (Load profile = 100 kW) .....	25
Table 6 PV2 measured parameters in MATLAB (Load profile = 100 kW) .....	25
Table 7 PV3 measured parameters in MATLAB (Load profile = 100 kW) .....	26
Table 8 PV4 measured parameters in MATLAB (Load profile = 100 kW) .....	27
Table 9 Measured parameters for P and Q (Load profile = 100 kW) .....	33
Table 10 Performance analysis of various resistive active load profiles .....	35
Table 11 Performance analysis of various resistive active and capacitive reactive load profiles connected in series .....	36
Table 12 Performance analysis of various resistive active and inductive reactive load profiles connected in series .....	36
Table 13 Performance analysis of various resistive active and inductive reactive load profiles connected in parallel .....	37
Table 14 Performance analysis of various resistive active and capacitive reactive load profiles connected in parallel .....	39

## LIST OF FIGURES

Figure 1 Methodology of the research .....	4
Figure 2 PV system classification .....	9
Figure 3 Topology of 400 kW grid-connected PV farm .....	14
Figure 4 MATLAB code used in the MPPT .....	17
Figure 5 Code diagram.....	18
Figure 6 Block parameters of capacitor bank in MATLAB/Simulink® .....	19
Figure 7 Block parameters of three-phase transformer in MATLAB/Simulink® .....	20
Figure 8 PV arrays and DC/DC boost converters connection topology .....	23
Figure 9 I-V and P-V characteristic curves.....	23
Figure 10 PV scopes connection topology.....	24
Figure 11 PV1 waveforms .....	25
Figure 12 PV2 waveforms .....	26
Figure 13 PV3 waveforms .....	26
Figure 14 PV4 waveforms .....	27
Figure 15 Topology of PV scope .....	27
Figure 16 Irradiance and mean power waveforms.....	28
Figure 17 PV arrays and boost converters connection topology .....	28
Figure 18 Expanded DC/DC boost convert block .....	29
Figure 19 Boost converters and VSC connection topology.....	29
Figure 20 Expanded VSC block.....	30
Figure 21 VSC main controller .....	30
Figure 22 Topology of VSC scopes .....	30
Figure 23 Vdc-ref and Vdc waveforms.....	31
Figure 24 VSC “m” value waveform .....	31
Figure 25 IdIq (pu) waveforms .....	31
Figure 26 VSC, three-phase transformer and VI measurement connection topology	32
Figure 27 Block parameters of three-phase transformer in MATLAB/Simulink® ....	32

Figure 28 Expanded three-phase VI measurement block ..... 32

Figure 29 PQ waveform generator circuit..... 33

Figure 30 Topology of VI PQ grid scope ..... 33

Figure 31 VI PQ waveforms ..... 33

Figure 32 RLC load block and utility grid connection topology ..... 34

# **I. INTRODUCTION**

## **A. Background**

For decades the electricity network was defined as a centralized and monodirectional system for electricity distribution. Power plants as structures for generating electricity were at one end of the power grid. There are three possible categories of power plants. Electricity generation in a thermal power plant happens by burning fuel to boil water to superheated steam that can run a turbine; nuclear power plants generate electricity by using the released heat produced from the fission of radioactive elements and, hydro-electric power plants produce electricity as the kinetic energy caused by falling water can drives turbines.

Generally, the power plants are located far from the consumers since huge amounts of land and water are needed, and an efficient transmission line is essential to transmit power from the plant to the load over long distances. As Tesla proposed, electricity is transmitted in a three-phase alternating current. In the power plants, the generated voltage is a high voltage between 50 and 150 kV. Therefore, at high voltage, and low current, the cable power dissipation is minimal. This high voltage must be decreased in the substation before reaching the consumer. The substation is in charge of switching, controlling, and protecting the electrical circuits. Electricity will then be distributed through the city network to reach the consumer. Power therefore moves from the plant to the user in one direction.

Since renewable energy (RE) sources are seen as a solution to climate change and are also becoming more affordable as a result of massive implementation and research expenditures, a more advanced network is required for their integration. Since Renewable energies can be produced on-site, new adaptations should be made for the transmission line. Decentralized systems should be replaced with the old versions to take into consideration the unpredictable nature of renewable energy sources (RES). Also, various energy storage systems can be employed to accommodate the demands

of the customers both during the day and at night.

In 2013 world's total renewable energy capacity was 1566487 MW. In 2020 this number increased to 2813159 MW as Asia has the most share with 1301702 MW, Europe in the second place with 609048 MW and North America in the third place with 422895 MW of cumulative electricity capacity. At the end of 2022 the world's cumulative electricity capacity reached to 3371793 MW where Asia, Europe and North America shared 1630282 MW, 708582 MW and 489226 MW of the cumulative electricity capacity. PV systems have a noticeable share of the given statistics. From 2013 world's Solar Photovoltaic capacity increased from 136572 MW to 1046614 MW in 2022 where Asia shares 596530 MW cumulative electricity capacity (IRENA, 2023).

As world's power generation continue to gain a higher share of renewable energies, new technologies and advanced systems are proposed and designed by the scientists. As sun is providing energy that can satisfy the electricity demand, an increased interest in exploring methods for utilizing this energy is rising. Silently generating energy can be considered as an advantage of using photovoltaic power generation. Meaning that no moving parts is needed in the generation process. Emission-free energy production can be accounted as another advantage when it comes to comparing the solar energy plant to a coal-fired plant. Also, solar energy is produced decentralized, enabling the users to consume energy at the same place.

The integration of renewable energy in the electrical network continues to be a difficulty, despite the significant role that solar energy is playing in the energy mix. Solar and Wind plants are located in a noticeable distance from the load; therefore, they require other components for high voltage transport. Small rooftop PV systems can also be installed in the building. In this case, the generated electricity must be able to flow and reach to the other consumers through the transmission lines while an energy storage in the building can be also used.

To add up, the future power grid must be a smart grid that can include and mix different energy sources, and be bidirectional and decentralized. It is therefore vital to understand the network merger of RE, classification and necessity of different systems and performance analysis of the systems.

## **B. Problem Statement**

Solar energy is available since the sun is always shining, but absorbing that energy and producing electricity efficiently, economically, and comprehensively remains a challenge. It has been seen in many projects that a lack of knowledge in system performance results in system failure and investment loss after a period of time. There is still much work required to improve the efficiency of the instruments and systems as the electricity demand and generation are increasing. Also, integration of the RE in the power grid has become an attractive area of research because the classic electricity network cannot fully support RE sources. To maintain the performance of the PV plants, compelling studies must be carried out to help better analysis and efficient design and installation. With a surge in PV energy technology, more detailed and meticulous analyses are also needed for systems to address the challenges and gaps.

## **C. Objective of The Research**

The last few decades have seen significant advancements in PV systems. Similar to them, modeling and analysis systems have made significant progress. Many of the new technologies that we see today have been created with the help of these systems, software, and simulators, to the extent that today it is possible to examine and analyze solar energy systems, different sites, the energy consumption and necessary systems in various regions of the world.

The main objective of this work is to simulate and analyze the performance of a grid-connected PV farm with a 400 kW capacity under different load conditions. Our objectives can therefore be restated as follows:

- Simulate the model in MATLAB/Simulink<sup>®</sup> and study the parameters.
- Study and analyze the system performance in every second of the simulation, and understand the effects of changing a parameter on the other parameters.
- Design different loads and test the system to understand and study the performance of the system.

- Define a valid performance range for the system.

#### D. Research Methodology

This section outlines the overview of the approach used in this work. The first part is focused on the literature review to create a basis for theoretical aspects. The second phase involved simulating the model and analyzing the system after collecting data. In the analysis process, parameters in the system were determined using MATLAB/Simulink<sup>®</sup>. The software made it possible for us to analyze the electrical behavior of the system, which can be seen graphically. Different scenarios were tested, and adjustments were made to validate the performance analysis. This study is based on grid-connected PV plant performance analysis and the valid performance range. Figure 1 shows the methodology of the research.

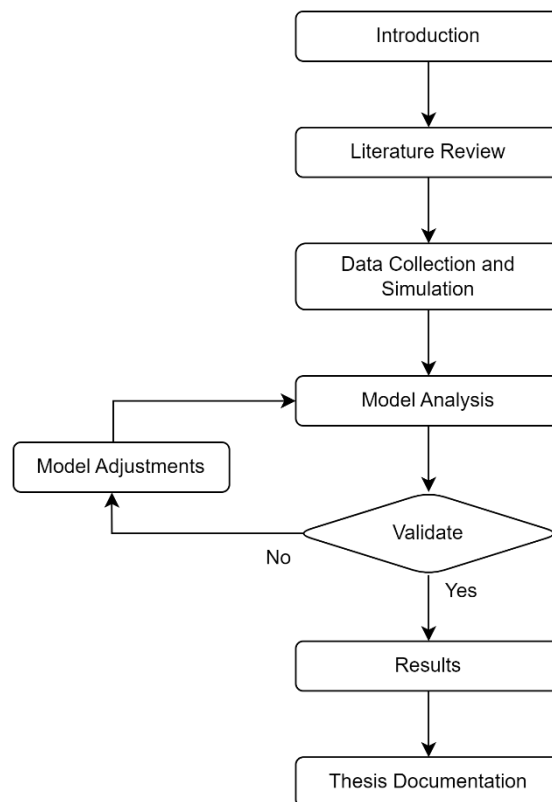


Figure 1 Methodology of the research

### **E. Scope of the Thesis**

This work deals with performance analysis a 400 kW grid-connected PV system using MATLAB/Simulink® software. The model is made up of four photovoltaic arrays with a capacity of 100 kW, DC/DC boost converters with individual MPPT controls, inverter, voltage source converter, load connected to the utility grid. The present investigation aims to analyze the system under resistive, capacitive, and inductive load conditions. Precisely, the primary purpose was calculating the system's valid performance range for various load conditions.

### **F. Significance of the Research**

Due to extensive industrial expansion, rising population, and ongoing increases in energy consumption, many nations worldwide are experiencing rising energy demand. It should be emphasized that electricity makes up the majority of the consumed energy. More electricity generation based on fossil fuels has resulted in environmental concerns. Therefore, RES are significant assets to fill the gap between demand and electricity generation in the following decades. Providing secure, sustainable, and clean energy is another reason for encouraging reliance on renewable sources. This study will contribute to enhancing the grid-connected PV system by analyzing system performance and behavior under different load conditions. The presented valid performance range can contribute to future studies and, along with the model, will result in a better understanding of the grid-connected PV systems, adjustment, and configuration of the components.

## **II. LITERATURE REVIEW**

### **A. Introduction**

We present a literature overview of the related works here. We briefly review the research done by scholars in different parts of the world.

HALABI et al. (2017) carried out research utilizing HOMER to analyze the performance of hybrid PV/diesel/battery systems. The location of the case study is in Sabah, Malaysia. To conduct the study, site surveys, and collected data were considered, and two decentralized power stations were analyzed that include a mix of PV, diesel generators, system converters, and energy storage. Operational behaviors of various photovoltaic penetration levels were studied to quantify the effect of the integration of the PV system. Technical, economic, and environmental aspects were analyzed. Also, changes in fuel, PV, battery prices, and electricity consumption were considered to help compare the different scenarios.

Performance assessment of a Hybrid Solar-Wind-Microhydro system was presented by MOSOBI et al. (2018). The integration of PV, wind energy, and microhydro systems was emphasized in the study with the help of simulation and performance analysis. Temperature, solar radiation, and speed of the wind were recognized as the variables for investigating the system's performance.

Some studies were carried out by JAVED et al. (2019) on a design and performance analysis of a Stand-alone PV System with Hybrid Energy Storage. The location of the study is rural India, where the domestic stand-alone PV system is proposed.

Research done by BHAN et al. (2021) showed Perturb and Observe concept used for the perturbation of the I-V curve step value. The study shows that value, including plus indication, can cause the perturbation to go in the opposite direction. More oscillations in the operating point of solar PV and a slower rate of convergence

are drawbacks of the P&O technology.

SURENDRA et al. (2022) carried out a study on analyzing a stand-alone PV system using the System Advisor Model. Many parameters, such as the monthly average of atmospheric pressure, dew point temperature, wind speed, direction, etc., were considered before the project's location selection. System advisor model tools were used in the study that can provide basic design for a power plant, such as average AC power estimation. Moreover, the article mentions that the prediction of the monthly irradiance values can result in more efficient load management.

SHAKIR et al. (2022) designed and performed a performance analysis on a stand-alone PV system located at Al-Nahrain University, Baghdad, Iraq. Designing and simulating a roof-top stand-alone PV system to generate electricity for the parking garage and laboratories can be considered the primary goal of this research. PVsyst6 was used to carry out the simulation and to aid in comparing four types of solar panels and estimating the shading effects. The financial analysis also was considered for economic feasibility.

CHABACHI et al. (2022) analyzed an experimental and simulated grid-connected PV system located in southwest Algeria. A grid-connected PV power plant with a rated capacity of 6 MW was simulated and tested during a specific time period. IEC 61724 helped analyze the system while data were collected on a daily and monthly basis from monitoring the system for two years. This study conducted a comparative study on the performance and PVsyst simulation results.

REHMAN et al. (2022) carried out a performance study on a grid-connected PV system located in Kuttiady village in Kerala, India. The main goal of this research is to present a techno-economic analysis including final yield, reference yield, performance ratio, benefit-cost ratio, and payback period. The study proposed a PV system that can generate more electricity than the village demand. The authors proposed that around 785 tons of greenhouse emissions might be prevented from entering the atmosphere at the location with the help of the proposed facility.

DESHMUKH and CHANDRAKAR (2022) conducted a detailed study on a grid-connected Solar PV system. Performance Forecasting Approach (PFA) is used for analysis where the location of the study is based on Mayo Hospital metro station,

Nagpur. The study includes the PV system's design, simulation, and analysis based on a daily output diagram, performance ratio, etc. The research offers a guideline for engineers and researchers engaged in solar PV power performance forecasting studies and a method for exploratory analysis.

A similar study was carried out by AMIR et al. (2022) on the performance analysis of a grid-connected hybrid system. In this study, factors such as adjusting MPPT, inverter, and multi-winding transformer reliability were investigated with the help of MATLAB software.

NARASIMMAN et al. (2023) investigate the real-time performance analysis and modeling of a grid-connected solar PV plant with 5 MW rated capacity study carries out the analysis using different artificial neural networks (ANN) such as Cascade forward backdrop, ELMAN back prop, Feed forward back prop and, etc. The impact of different environmental parameters on power production is measured in this study.

## **B. PV System Classification**

Photovoltaic systems can be classified into three main categories; grid-connected, stand-alone, and hybrid, as displayed in Figure 2. The main factors for this categorization are the system's configuration, function, and connection topology. The two main categories are grid-connected and stand-alone PV systems. Grid-connected PV systems can directly connect to the load with or without energy storage. Stand-alone PV systems can integrate battery storage for DC mode and inverter in case of an AC load. Hybrid PV systems are a mix of PV panels with either renewable or non-renewable energy sources (MADETI, 2017; ASSADEG, 2019).

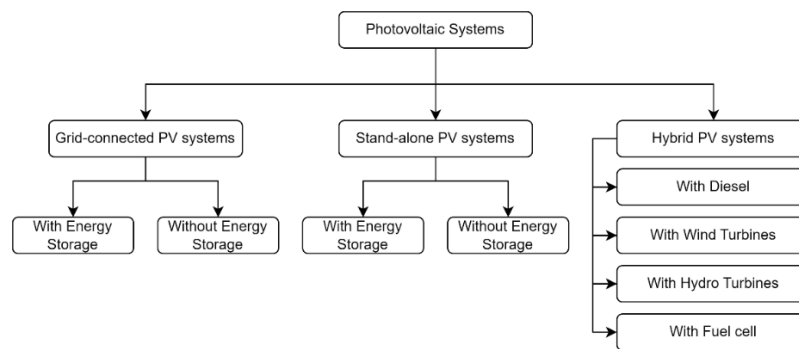


Figure 2 PV system classification

## 1. Grid-Connected PV System

In a grid-connected PV system, solar photovoltaic modules work as the electricity generators while the inverter works as the converter and DC power controller, which can deliver the power to the grid with the help of other devices in the system. Photovoltaic modules, DC/AC junction box, power conditioning unit (PCU), the AC distribution board, the transformer, and other control and isolating devices are considered essential components of a grid-connected PV system. PV systems made it possible to use them in a variety of applications from small residential to large scale and megawatt level bases. The power generated by the PV system can be fed to the grid in the presence of sunlight, while the system can operate with or without energy storage. IEA reports demonstrate that solar PV power generation reached 942 GW by the end of 2021, regardless of the difficulties brought on by the COVID-19 pandemic (IEA, 2022); and continued to grow and reach 1185 GW of cumulative capacity in 2022 (IEA, 2023).

Grid-connected PV systems can divide into three subcategories (MADETI, 2017; SATPATHY, 2020):

- Ground-mounted, grid-connected solar PV power plants
- Roof-mounted, grid-connected solar PV power plants
- Building-integrated, grid-connected solar PV power plants

### 1.1. Components of a Grid-Connected PV System

Primary elements of a grid-connected PV system can be defined as solar PV modules, DC Array Junction Box (String Combiner Box), Inverter/Power

Conditioning Unit, AC Distribution Board, DC and AC Cable, HT cable, Module Mounting Structure, Single Axis Tracker (optional), Transformer, Isolators, LT Panel, Switchgear/HT Panel, HT Switchyard/Substation, and Metering Unit.

A string is needed to get the required voltage from the system, consisting of modules connected in series. The combiner box includes the combined number of strings connected in parallel where the output is connected to the inverter input. The inverter's MPPT gets the maximum power point of each array, while the inverter itself converts the DC power into AC power (three-phase AC power). The output of the inverter will be stepped up depending on the system requirements with the help of an inverter duty transformer. Switchgear that includes the combined transformer output in a parallel form will transmit the power to the switchyard, where power is evacuated to the transmission line. SCADA systems are necessary to monitor and control the parameters of a facility (SATPATHY, 2020).

## **1.2. Design of a Grid-Connected PV System**

Designing a grid-connected PV plant requires a deep understanding of parameters such as the latitude and longitude of the desired site, the available area, the required capacity, requirements of the generation, and PLF/CUF values as PPA, voltage of power evacuation, and transmission line distance. A feasible study on designing a grid-connected PV system must contain site surveys, techno-economic, framework logistics, data and solar radiation analysis, choosing proper module and inverter, design of the string, designing the structure of the module mounting, tilt angle, ratio of DC to AC, interrow spacing, shadow assessment, making of layout, DC cable design, AC distribution board or LT panel, energy yield estimation, design earthing, lightning arrester design and connection, auxiliary power supply – transformers, grid connection, transformer, HT panel, circuit breakers, protection, metering and control cubicles, lightning arrestors, isolators and insulators, and weather monitoring station (SATPATHY, 2020).

## **2. Stand-Alone PV System**

Stand-alone PV systems, or off-grid PV systems, are systems without connection to the power grid. Directly coupled systems can be connected directly to the load where the generated power will supply the load in sunlight. An MPPT can be

connected between the PV arrays and the load for better system utilization. Other stand-alone PV systems with energy storage can supply AC and DC loads when there is no sunlight. In such systems, few components are required, such as a charge controller which can regulate the PV array's output current. A dual DC cut-off switch can guarantee system security during faulty conditions. More precisely, these systems are a good choice in areas without electricity supply, energy shortage, or remote locations where the power grid is not accessible (MADETI, 2017; SATPATHY, 2020).

### **2.1. Components of a Stand-Alone PV System**

In a stand-alone PV system, solar PV modules are connected in series to form strings. An array junction box contains the combined strings and is placed near the PV arrays. The generated DC electricity flows from the PV panels to the inverter, passing through the array junction box (string combiner box). The controller manages the batteries' DC power. The AC electricity converted by the inverter goes to the main electrical panel where loads can be supplied. Solar PV modules, solar charge controller, battery, off-grid/hybrid inverter, mounting structures of the PV modules, array junction box, AC distribution board, and DC and AC cables are the main components of a stand-alone PV system (SATPATHY, 2020).

### **2.2. Design of a Stand-Alone PV System**

The primary considerations in designing a PV system can be defined as follow. The daily energy requirement is an essential factor that can be estimated on a monthly basis to match the daily energy production. The desired DC voltage value is vital in choosing the system components. This can directly rely on the module or array's capacity, solar charge controller, battery, and inverter operational voltage. The energy availability at the battery with a specific load curve and period for optimal size determines the loss of load probability (LOLP) of a standalone or off-grid solar PV system. The time percentage that a solar PV system can meet the load's energy supply is the system availability which is directly connected to the battery's capacity. A higher battery capacity results in higher system availability and also increases system costs. The highest achievable efficiency can be calculated as a multiplier of the system components' efficiencies. Thus, component selection is crucial in the design process. Cost optimization is another important aspect in designing a stand-alone PV power

system, where the customer's expectations are considered. While taking system availability into account, there should be a balance between the overall optimized cost and the solar PV system's optimized performance (SATPATHY, 2020).

### **3. Hybrid PV System**

Hybrid systems generally refer to the combination of a PV system integrated with any conventional or non-conventional energy sources. In such systems, electricity generated by the PV system will supply the load as the alternative energy source will be used when the demand reaches the peak value. Hybrid systems are considered reliable supplies with low operation and maintenance costs (MADETI, 2017). Hybrid solar PV power systems with battery storage normally employ more than one renewable energy supply source. A hybrid solar and wind farm can be assumed as an example. In such a system, the generated electricity would charge the battery and supply the load (SATPATHY, 2020; SUMATHI, 2015).

#### **C. Grid Integration of Solar PV Systems**

The integration of a solar PV system into the grid is considered very important. The integration level depends on the scale of generation. Meaning that the PV system can be integrated into the grid at the distribution or transmission level. Studies show that some steps can be defined to describe the grid integration process of a PV power system (SATPATHY, 2020).

- Step 1: To provide the necessary DC voltage (within the range of the inverter's DC input), the solar array has to be interconnected.
- Step 2: Grid management feature considerations, such as Reactive power support, islanding, etc., must be approved.
- Step 3: The range grid parameters have to be within the inverter operation range.
- Step 4: Comparing voltage and frequency with the grid characteristics while switching DC and AC breakers.

Integration of small solar PV power, hydro, biogas, biomass, and small wind turbine power generators can be considered as small-scale integration. Generally, the generated power varies between a few hundred kilowatts to several megawatts.

Distributed resources (DR) are defined as the place of the connection between the grid and small-scale power generators that can have both renewable and non-renewable resources (SUMATHI, 2015).

The integration of large-scale renewable energy generations, such as hydro and steam turbines operated with biomass or geothermal energy, is familiar to the grid, while the integration of large-scale wind energy power generators is challenging because of the irregular nature of the wind (SUMATHI, 2015).

There are some requirements for grid integration, which can be described as the range of grid voltage and range of grid frequency, harmonics on the AC side, voltage unbalance, power quality, and fault ride through.

The range of grid voltage and range of grid frequency has to be in the range of the inverter. This voltage and frequency are monitored by the inverter. The system will be disconnected if the values are out of the required range. Some loads cause harmonic distortion. The harmonics on the AC side is the value for the harmonic limitation defined by the grid code. The deviation between the maximum and minimum line voltages divided by the average value of the line voltage is the voltage unbalance value. The proper voltage unbalance value of the PV plants should not exceed 2% for at least 30 seconds. The highest occasional fluctuations permissible limit for voltage can be defined as 3% and 1% for the repetitive fluctuations. The PCU is responsible for the power quality of the system, where IEC 61727 defines the value of the DC injection range by 1% of the rated current of the inverter. As per IEC 61000-3-7, the range of the flicker produced by the PV plant has to be greater or equal to 0.35 over the time periods of 2 hours and greater or equal to 0.25 for the time periods of 10 minutes. Additionally, Fault ride through can be interpreted as the solar PV plant's ability to ride through the grid fault when the voltage drops temporarily (SATPATHY, 2020; SUMATHI, 2015).

### III. MODELING OF GRID-CONNECTED PV SYSTEM

#### A. Introduction

In this work a grid-connected PV system with capacity of 400 kW was simulated. Components of the system are described and related graphical curves are presented. Modeling of the system is available under “Examples” in MathWorks Inc. Two main sections of this system can be considered as the PV power generator and the utility grid connected to it.

#### B. System Overview

Figure 3 demonstrates the system topology in the environment of the MATLAB/Simulink<sup>®</sup> software. The presented PV farm includes four PV arrays that together can generate 400 kW. A DC/DC converter controlled by individual MPPT is connected to each of the PV arrays. A DC bus of 500 V is used in the system. The system consists a three-phase VSC with capacity of converting 500 V DC to 260 V AC. To connect the converter to the power grid a three-phase coupling transformer is used. Distribution feeders and equivalent transmission system are modeled as the utility grid.

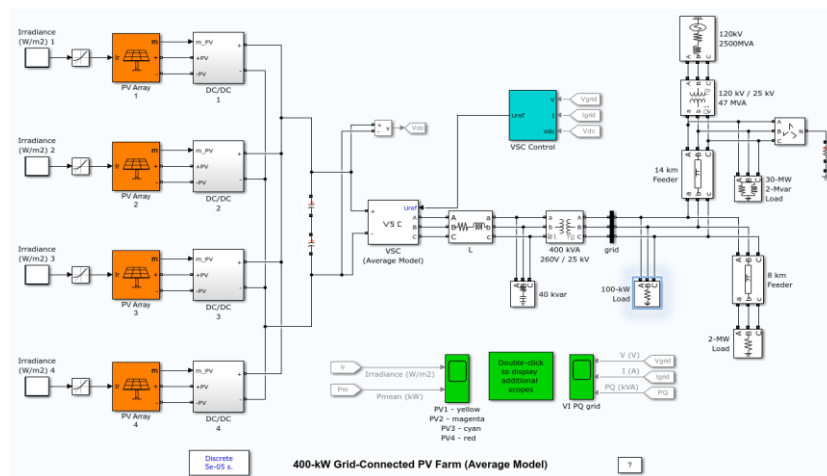


Figure 3 Topology of 400 kW grid-connected PV farm (MATHWORKS)

## C. Modeling of System Components

### 1. PV Array

Solar PV modules may be divided into monocrystalline and multicrystalline groups based on their size, cost, technology, and wattages. BSF standard and poly-*PERC* type are available for the multi crystalline group while for line solar cell category, standard Al-BSF-based p-type, p-type *PERC*, n-type *IBC*, *HJT/HIT*, *PERT*, and *PERL* cell-based modules are available in the mono crystalline category. Other solar modules, such as half-cut cell technology-based and bifacial cell-based modules, are also available (SATPATHY, 2020).

In this study, four PV arrays make the presented PV farm. Each of the 64 parallel strings in a single PV array block has five SunPower SPR-315E modules that are connected in series. Table 1 shows the technical specifications of the SunPower SPR-315E module. Model parameters for the module are demonstrated in Table 2.

Table 1 Technical Specifications of SunPower SPR-315E module

Cell Type	Mono
Number of cells per module Ncell	96
Maximum power (W)	315.072
Open circuit voltage Voc	64.6
Current at maximum power point Imp	5.76
Short-circuit current Ics	6.14
Voltage at maximum power point Vmp	54.7
Temperature coefficient of Voc	-0.2727
Temperature coefficient of Isc	0.061743
Temperature coefficient of maximum power	-0.386
Nominal Operating Cell Temp (°C)	46.0
Power at STC (Standard Test Conditions)	315
Power at PTC (PVUSA Test Conditions)	290
Power Density at STC (W / m <sup>2</sup> )	193.252
Power Density at PTC (W / m <sup>2</sup> )	177.914
Module area (m <sup>2</sup> )	1.63

Table 2 Model parameters for SunPower SPR-315E

Light-generated current IL (A)	6.1461
Diode saturation current I0 (A)	6.5067e-12
Diode ideality factor	0.95071
Shunt resistance Rsh (ohms)	430.0666
Series resistance Rs (ohms)	0.43041

The PV Array block in MATLAB/Simulink<sup>®</sup> is a five-parameter model with irradiance and temperature as the inputs, measurements as output, and specialized electrical conserving ports (positive and negative). The output of the PV arrays is connected to individual DC/DC converters.

## 2. DC/DC Boost Converter

DC/DC boost converters are widely used components. Changes in solar irradiance and temperature can cause voltage fluctuation in PV arrays. The unregulated DC voltage obtained by the PV array is considered the converter's input. In the boost converter, the input voltage changes, yet the output has to be controlled. From the energy perspective, continuously adjusting the absorbed energy received from the source and the injected energy to the load enables the boost converter to regulate the voltage. The process of energy absorption and injection serves as a switching cycle. Meaning that an idling period is needed for the injection intervals. Two modes can be defined for the converters; discontinuous conduction and continuous modes. Factors such as the capacity of the energy storage and switching period affect choosing the mode of the converter (HASANEEN, 2008).

In this study, four DC/DC boost converters are connected to the PV arrays. The converters are linked to a 500 V common DC bus. Each boost is controlled by an individual MPPT. The "Perturb and Observe" MPPT approach was chosen because it can change the voltage across the PV terminals.

### 2.1. Control Strategy

The individual MPPTs in the converters are accounted for to maintain the operating point and assist the system in getting the maximum power point from the PV arrays. In this study, "Perturb and Observe" (P&O) is selected as the control method. This technique allows the voltage to be controlled by adjusting the duty cycle. In every cycle, the power obtained by the PV array is compared with the previous cycle. The rate of current is also determined by this method. Figure 4 shows the MATLAB code used in the MPPT.

Code starts by defining the function's name (PandO), which is the name of the technique used in the MPPT. Then Param, Enabled, V and I are defined as the inputs for the function. D represents the duty cycle which is a scalar value returned by the function. Next, Dinit, Dmax, Dmin and deltaD are initialized using Param. These variables will assist the function in controlling the rate change of the duty cycle. The next step is to initialize the persistent variables of the PV array's terminal voltage, power and duty cycle (Vold, Pold and Dold). Meaning that the function can call these

valuables when needed. After that, the code will assign default values to persistent variables, which are 0 for Vold and Pold and Dinit for the duty cycle. Changes in voltage and power are calculated afterward to specify the changes in the duty cycle. The block code of the P&O algorithm implementation comes after the code checks the changes in the power value (non-zero value) and the MPPT controller's status. If the power changes are not zero and the MPPT is enabled, it checks whether the change in power and terminal voltage is positive or negative. In response to these circumstances, it changes the duty cycle (D) by deltaD. The duty cycle is returned to its initial value (Dold) if the change in power is zero or the MPPT controller is disabled.

```
function D = Pand0(Param, Enabled, V, I)

% MPPT controller based on the Perturb & Observe algorithm.

% D output = Duty cycle of the boost converter (value between 0 and 1)
%
% Enabled input = 1 to enable the MPPT controller
% V input = PV array terminal voltage (V)
% I input = PV array current (A)
%
% Param input:
Dinit = Param(1); %Initial value for D output
Dmax = Param(2); %Maximum value for D
Dmin = Param(3); %Minimum value for D
deltaD = Param(4); %Increment value used to increase/decrease the duty cycle D
% ( increasing D = decreasing Vref )
%

persistent Vold Pold Dold;

dataType = 'double';

if isempty(Vold)
    Vold=0;
    Pold=0;
    Dold=Dinit;
end
P= V*I;
dV= V - Vold;
dP= P - Pold;

if dP ~= 0 & Enabled ~=0
    if dP < 0
        if dV < 0
            D = Dold - deltaD;
        else
            D = Dold + deltaD;
        end
    else
        if dV < 0
            D = Dold + deltaD;
        else
            D = Dold - deltaD;
        end
    end
else D=Dold;
end

if D >= Dmax | D<= Dmin
    D=Dold;
end

Dold=D;
Vold=V;
Pold=P;
```

Figure 4 MATLAB code used in the MPPT

The next step is to find whether the duty cycle (D) is within the specified range of Dmax and Dmin. If the value is out of the range, the previous value of the duty cycle

(Dold) will be set. To update the persistent variables (Dold, Vold and Pold), the code will assign new values to them. And they will be used in the next call of the function. And finally, the output of the MPPT controller will be available. The code diagram is shown in Figure 5.

Using Perturb & Observe technique can be beneficial because of its simple structure, easy implementation, low cost, and comparatively accurate method. When there are a lot of variances in sun irradiation, this technique is not appropriate. Additionally, the voltage never truly hits a precise amount but instead perturbs near the maximum power (ELMELEGI and AHMED, 2015).

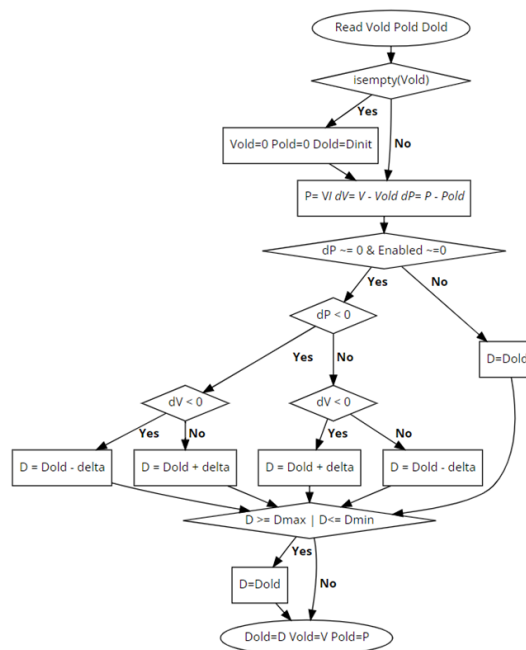


Figure 5 Code diagram

### 3. Voltage Source Converter

To interlink DC and AC systems, a three-phase voltage source converter (VSC) is used. The three-phase VSC is often used in electric car charging stations, traction motor drives for transportation applications, solar and wind energy systems, battery storage grid integration, etc. (SRITA, 2022).

VSC's structure can be categorized into power stage, switching signal generation, and discrete-time control system. The outer control loops are the DC bus voltage control and active/reactive power control, which can generate the reference

grid current for the inner current control loop. To track the reference and to ignore low-frequency harmonics in the voltage of the grid, the grid current is necessary.

Typically, harmonic controllers are connected to the current controller. The most popular methods for mitigating the grid voltage harmonics are multi-resonant controllers, repetitive controllers in the stationary reference frame, and multiple synchronous reference frame control. In addition, the capacity to adjust to changing grid frequencies is necessary to maintain control performance. To generate the switching signals for VSC's semiconductor switches, a switching signal is needed, which is created by the pulse width modulation (PWM) unit using duty ratios. Today, a microcontroller or a digital signal processor (DSP) can implement the control scheme of the three-phase VSCs and other power converters (SRITA, 2022).

In the presented grid-connected model, a three-phase VSC is used to convert 500 V DC to 260 V AC while keeping a unity power factor.

#### 4. Capacitor Bank

To improve the power factor of the system, a capacitor bank is modeled. Capacitor bank adds reactive power the system. Therefore, designing them requires reactive power calculation in the system. In this study, the capacity of the capacitor bank is 40 kvar which is suitable to filter the harmonics produced by the VSC (KALHARI, 2022). Figure 6 shows the block parameters of the capacitor bank used in the system.

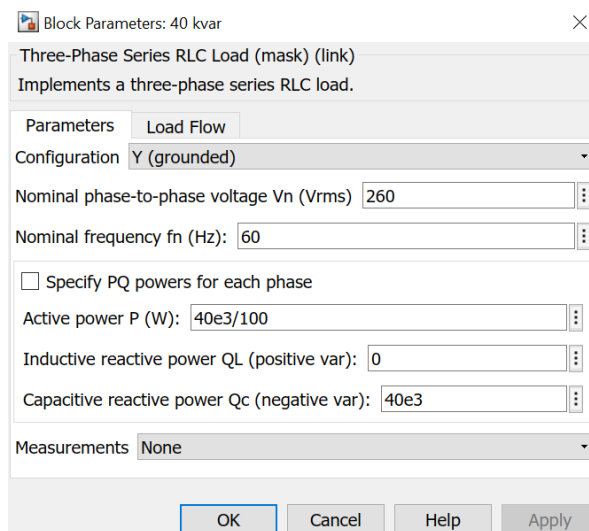


Figure 6 Block parameters of capacitor bank in MATLAB/Simulink®

## 5. Coupling Transformer

Modeling the system transformer is an important task that assists the designer with equipment selection, impact evaluation of various transients on the power quality, and choosing compensating devices. Calculating parameters for transformer modeling should be in accordance with the technical specifications of domestic power equipment manufacturers. An equivalent circuit must be used in the modeling process in which the electromagnetic couplings are replaced by electrical ones. The T-shaped equivalent circuit is more accurate but less practical for manual computations. In MATLAB, a transformer is modeled using the technique mentioned (BELOV, 2022). This study presents a three-phase coupling transformer, which can connect the converter to the power grid. The capacity of the transformer is 400 kVA 260 V/25 kV. Figure 7 shows the block parameters of the three-phase transformer (two windings) used in the study.

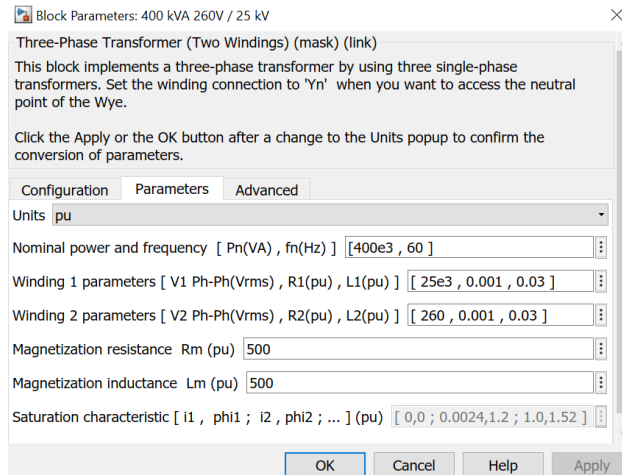


Figure 7 Block parameters of three-phase transformer in MATLAB/Simulink®

## 6. RLC Load Block

To simulate the power consumption in the system, RLC load blocks are used. In this study, a three-phase series RLC load block and also, a three-phase parallel RLC load block is used. Both implement a three-phase balanced load. However, they are different in connection topology. The load flow tab consists of parameters that are just used for initializing the model. In this study, "constant Z" is selected for the load type under the load flow tab. Nominal phase-to-phase voltage, active and reactive power determine the impedance of the load. As it is mentioned in the simulation results and discussion section, performance analysis of the system under different load conditions

is carried out in this study. Meaning that different adjustments will be made on one of the load blocks.

## **7. Utility Grid**

A typical North American grid is selected to be modeled in the system. The grid includes a 25 kV distribution feeder and 120 kV equivalent transmission system.

## IV. SIMULATION RESULTS AND DISCUSSION

### A. Introduction

This section presents the analysis report and main findings of the work. The 400 kW grid-connected PV farm is modeled in the MATLAB/Simulink® R2021b environment. The boost and VSC converters are represented in this model by equivalent voltage sources that produce the AC voltage averaged across one switching frequency cycle. While dynamics resulting from the control system and power system interaction is preserved, harmonics are not represented by this model. The simulation runs substantially fast because a time step of 50 us is used.

### B. System Simulation

As mentioned earlier, the PV power generation system includes four PV arrays, each of which consists of 64 parallel strings, including five series-connected modules per string. The selected module is SunPower SPR-315E, with the ability to deliver a maximum of 100 kW at 1000 W/m<sup>2</sup> sun irradiance. Figure 8 shows the PV arrays' connection to the DC/DC boost converters. The technical specification and module parameters are shown in Tables 1 and 2.

From the right, an individual stair generator connected to a rate limiter is used for the PV arrays' input irradiance value. To simulate the shading resulted by the clouds in the sky, different matrix for time and amplitude of the irradiance is set for each of the PV arrays which is shown in Table 3.

Table 3 PV arrays' matrix for time and amplitude of the irradiance

PV Array	Time (s)	Amplitude
PV1	[0, 0.5, 2.3]	[0, 0.05, 1.0]*1000
PV2	[0, 1.5, 2.2]	[0, 0.2, 1.0]*1000
PV3	[0, 0.5, 1.5]	[0, 0.6, 1.0]*1000
PV4	[0, 1, 2.0]	[0, 0.35, 1.0]*1000

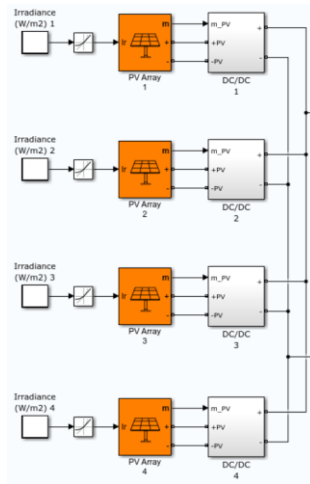


Figure 8 PV arrays and DC/DC boost converters connection topology

Table 4 lists the operating temperature and measured parameters for each PV array.

Table 4 Measured parameters for PV arrays with respect to the given temperature in robust discrete model

PV array	Temperature °C	Isc (A)	Vmp (V)	Imp (A)	Voc (V)	Pm (W)
PV1	40	396.599	259.495	370.885	309.788	96242.6
PV2	45	397.812	254.955	371.424	305.384	94696.2
PV3	35	395.386	264.036	370.322	314.192	97778.3
PV4	45	397.812	254.955	371.424	305.384	94696.2

Using the robust discrete model for the PV arrays cause the I-V and P-V characteristics curves to be different from each other. This option is available under “Advanced Parameters” tab in the software, which causes the algebraic loop within the PV array to break. Meaning that better performance can be expected from powergui. As it is mentioned in Table 4, a constant temperature will be set for each of the PV arrays. I-V and P-V characteristic curves for each of the PV arrays are illustrated in Figure 9.

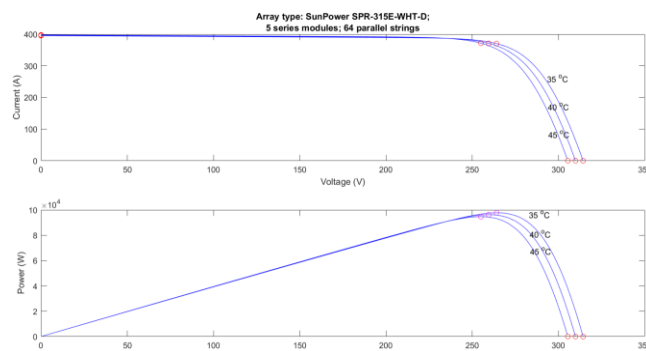


Figure 9 I-V and P-V characteristic curves

Figure 10 displays the PV scopes and their inputs. “Ir” as the irradiance and “Pm” as the mean power can be seen at the bottom of the figure. These parameters derived from the PV arrays are later used for analyzing power changes at different irradiance values.

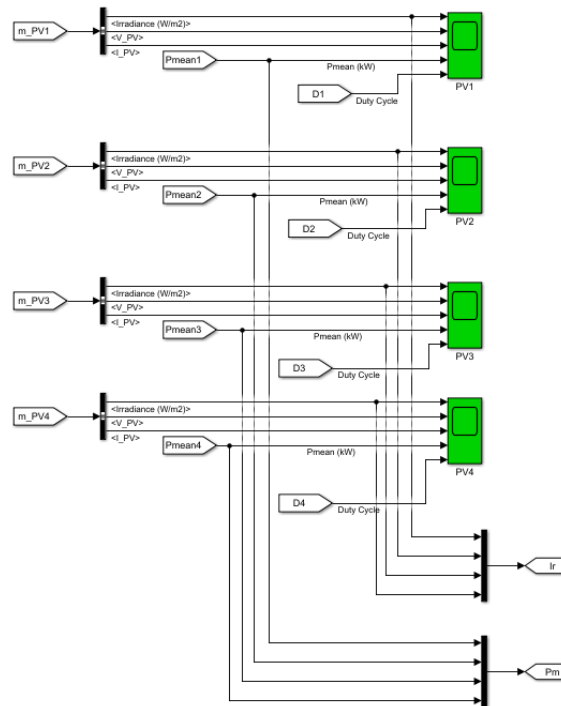


Figure 10 PV scopes connection topology

The irradiance value of PV1 is  $1000 \text{ W/m}^2$ . In  $0.5^{\text{th}}$  second this value drops to  $50 \text{ W/m}^2$  and comes back to  $1000 \text{ W/m}^2$  in  $2.3^{\text{rd}}$  second. This can simulate the presence of clouds in the sky. Table 5 shows the measured parameters for PV1. It is seen from the table that in  $0.622^{\text{nd}}$  second irradiance is  $50 \text{ W/m}^2$  where the lowest current value is measured (12.9 A). In the  $2.3^{\text{rd}}$  second, irradiance increases until in the  $2.42^{\text{nd}}$  second, it reaches  $1000 \text{ W/m}^2$ . Current at this point has the highest value (387.5 A). The observations also agree that the MPPT is working correctly since the voltage is stable. As the simulation duration is 3 seconds, in the  $3^{\text{rd}}$  second, all of the parameters are back to default values. Figure 11 demonstrates the PV1 waveforms. It can be seen that the generated power drops from 96.2 kW to 4.3 kW caused by the current decrease in the simulation time period.

Table 5 PV1 measured parameters in MATLAB (Load profile = 100 kW)

Time (s)	Irradiance (W/m2)	Voltage (V)	Current (A)	Pmean (kW)	Duty Cycle
0	1000	298	153.5	100	0.48
0.5	1000	260.7	368.8	96.2	0.48
0.622	50	259.1	12.9	8.2	0.47
2.3	50	235.2	18.5	4.3	0.53
2.420	1000	232.6	387.5	87.7	0.55
3	1000	260	369	96.2	0.48

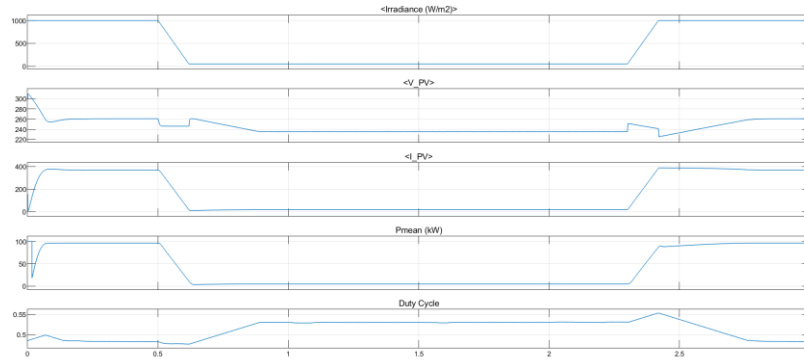


Figure 11 PV1 waveforms

PV2 is set to have an irradiance value of 1000 W/m<sup>2</sup> at the beginning of the simulation, 200 W/m<sup>2</sup> in the 1.5<sup>th</sup> second and 1000 W/m<sup>2</sup> in the 2.2<sup>nd</sup> second to simulate the presence of clouds. Table 6 and Fig 12 shows the measured parameters and PV2 waveforms. Irradiance starts to slightly reach 200 W/m<sup>2</sup> in the 1.6<sup>th</sup> second. During this time, the current drops from 369.4 A to 75.1 A. This affects the power value to decrease from 94.6 kW in the 1.5<sup>th</sup> second to 24.4 kW in the 1.6<sup>th</sup> second. Then, in 2.199 to 2.301<sup>st</sup> second, the irradiance increases to 1000 W/m<sup>2</sup>. Voltage changes are not considered since the MPPT controller functions efficiently by adjusting the duty cycle.

Table 6 PV2 measured parameters in MATLAB (Load profile = 100 kW)

Time (s)	Irradiance (W/m2)	Voltage (V)	Current (A)	Pmean (kW)	Duty Cycle
0	1000	294	145.9	100	0.49
1.5	1000	256	369.4	94.6	0.49
1.6	200	242	75.1	24.4	0.48
2.199	200	244	74.4	18.2	0.51
2.301	1000	268.3	339.4	85.4	0.49
3	1000	256.3	369.3	94.6	0.49

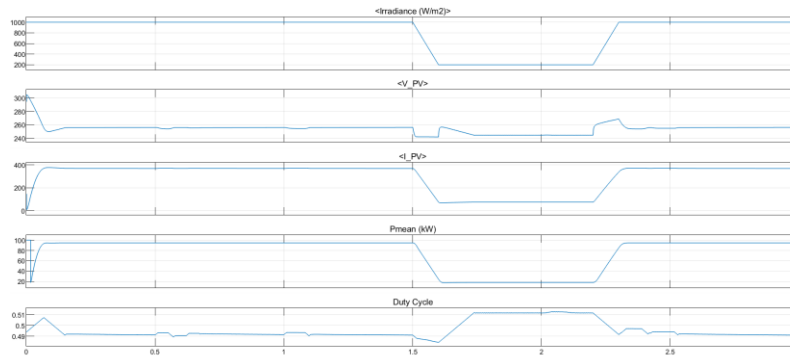


Figure 12 PV2 waveforms

The irradiance value of PV3 is set to be 1000 W/m<sup>2</sup> in the 0 second, 600 W/m<sup>2</sup> in the 0.5<sup>th</sup> second and comes back to 1000 W/m<sup>2</sup> in the 1.5<sup>th</sup> second to demonstrate clouds in the sky. As Table 7 shows the measured parameters of PV3, the irradiance reaches 600 W/m<sup>2</sup> in the 0.553<sup>rd</sup> second. Current value drops because of the drop in irradiance value. But the voltage is not changing so much since the duty cycle is being adjusted by the MPPT. In the 1.498<sup>th</sup> second current with 221.4 A and power with 58.4 kW are at their minimum values because the irradiance value is 600 W/m<sup>2</sup>. However, the voltage value is 263.9 V, with a slight change from the beginning of the simulation. After that, the irradiance starts to come back to 1000 W/m<sup>2</sup>. Figure 13 displays the PV3 waveforms.

Table 7 PV3 measured parameters in MATLAB (Load profile = 100 kW)

Time (s)	Irradiance (W/m <sup>2</sup> )	Voltage (V)	Current (A)	Pmean (kW)	Duty Cycle
0	1000	302.8	154.8	100	0.47
0.5	1000	265.4	368.2	97.7	0.47
0.553	600	261.2	223.6	61.8	0.46
1.498	600	263.9	221.4	58.4	0.47
1.55	1000	280.7	326.4	86	0.46
3	1000	265.5	368.2	97.7	0.47

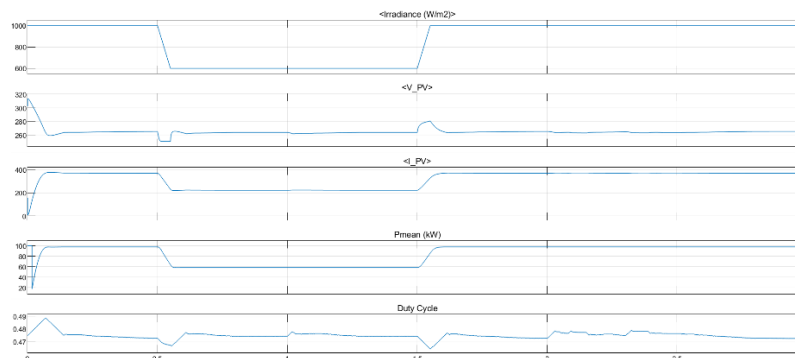


Figure 13 PV3 waveforms

The irradiance value for PV4 is set to be 1000 W/m<sup>2</sup> from 0 to 1<sup>st</sup> second. Then the irradiance decreases and reaches 350 W/m<sup>2</sup> in the 1<sup>st</sup> second and comes back to the initial value in the 2<sup>nd</sup> second to show the effects of having clouds. As can be observed from Table 8 and Figure 14, irradiance reaches 350 W/m<sup>2</sup> in the 1.084<sup>th</sup> second after a slight decrease. This causes the power to drop to 36.6 kW at that point. The system experiences the lowest power value of 32.5 kW in the 1.999<sup>th</sup> second while the irradiance is 350 W/m<sup>2</sup>. In the 2.082<sup>nd</sup> second, the irradiance gets to 1000 W/m<sup>2</sup> and stays at this value until the end of the simulation time. MPPT is working properly by varying the duty cycle to assist in stabilizing the voltage.

Table 8 PV4 measured parameters in MATLAB (Load profile = 100 kW)

Time (s)	Irradiance (W/m <sup>2</sup> )	Voltage (V)	Current (A)	Pmean (kW)	Duty Cycle
0	1000	294.5	145.9	100	0.49
1	1000	256.1	369.7	94.6	0.49
1.084	350	252.6	128.6	36.6	0.48
1.999	350	249.3	130.5	32.5	0.50
2.082	1000	270.6	330.9	83.9	0.48
3	1000	256.3	369.3	94.6	0.49

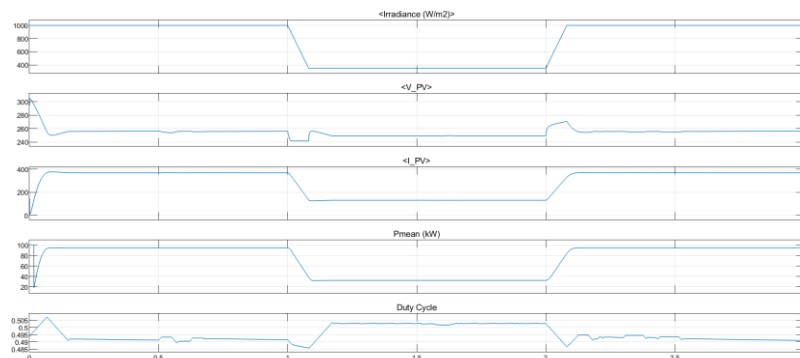


Figure 14 PV4 waveforms

As mentioned earlier, Ir and Pm are derived from PV arrays to help analyze power changes at different irradiance values. Figure 15 displays the PV scope containing the irradiance and power values of the PV arrays.

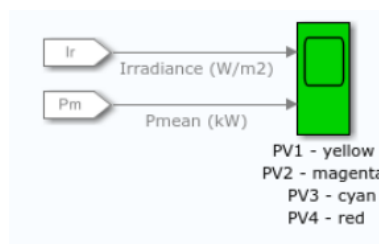


Figure 15 Topology of PV scope

Figure 16 shows the irradiance and power waveforms. It is evident that changes in power values are resulted from changes of solar radiation.

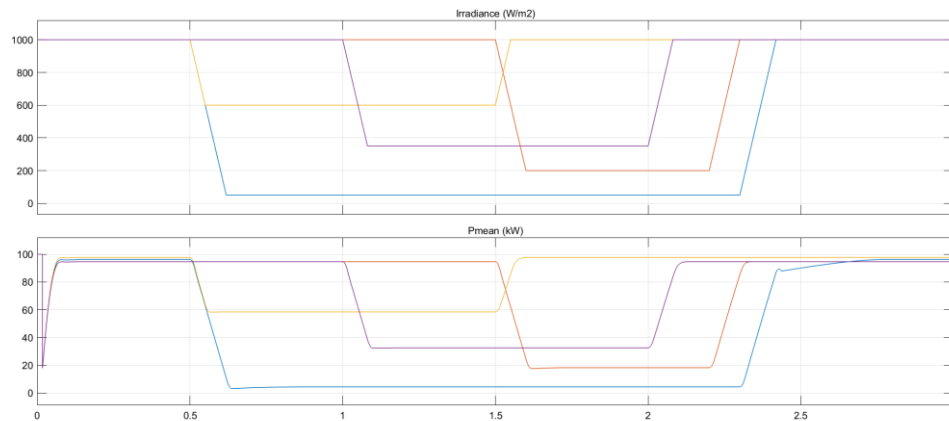


Figure 16 Irradiance and mean power waveforms

As it is shown in Figure 17, the outputs of the PV arrays are connected to individual DC/DC boost converters. These converters are connected to a common DC bus of 500 V. An individual MPPT is used in the converters, which can operate using the P&O approach, to regulate each boost converter.

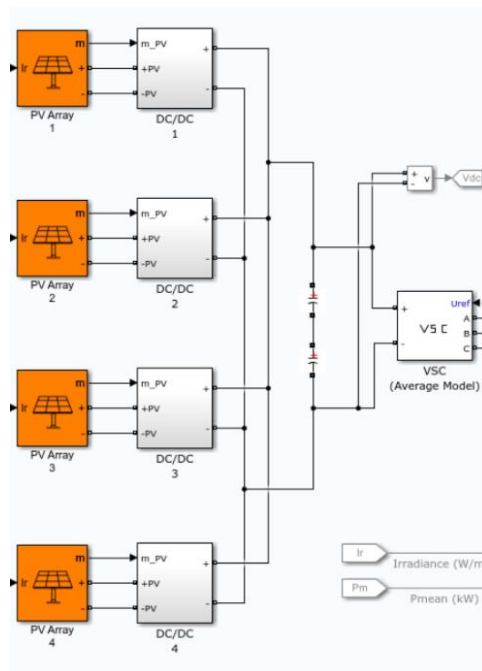


Figure 17 PV arrays and boost converters connection topology



Figure 20 shows the expanded VSC block. This block is an average model VSC with three bridge arms. Figure 21 shows the VSC main controller and VSC scopes are displayed in Figure 22.

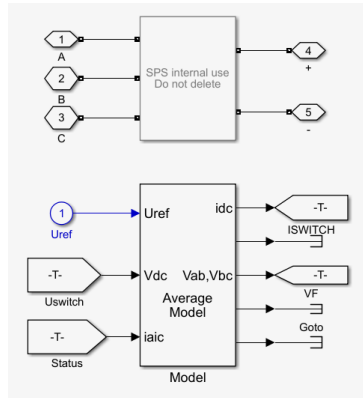


Figure 20 Expanded VSC block

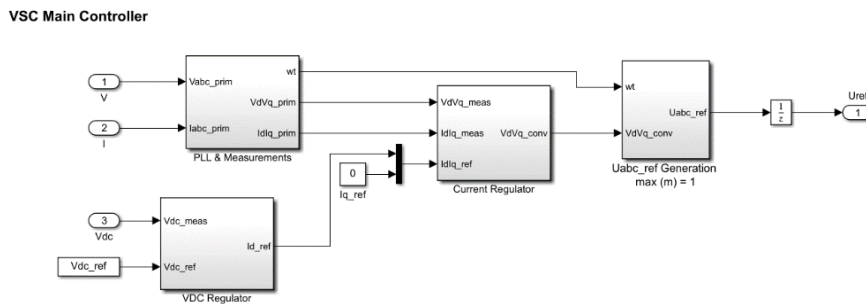


Figure 21 VSC main controller

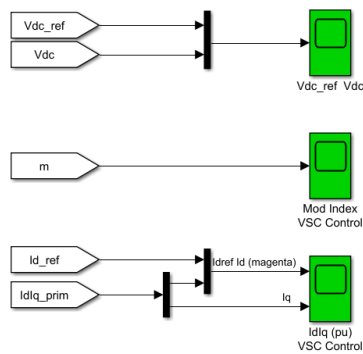


Figure 22 Topology of VSC scopes

Figure 23 demonstrates the Vdc-ref and Vdc waveforms. Vdc can be calculated as the sum of VSC's negative and positive voltage values. Vdc changes can be attributed to the irradiance changes of the PV arrays. Vdc-ref waveform is based on the VDC Regulator data in the VSC control block.

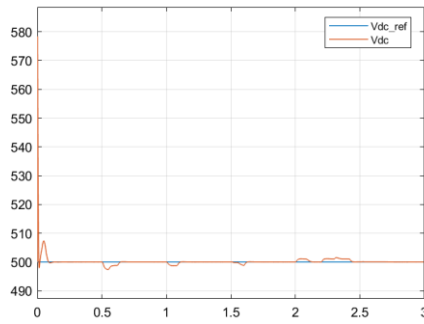


Figure 23 Vdc-ref and Vdc waveforms

The Mod index of the VSC control is shown in Figure 24. The waveform graphically shows the changes in the “m” value where the upper limit is 1 and the lower limit is 0.

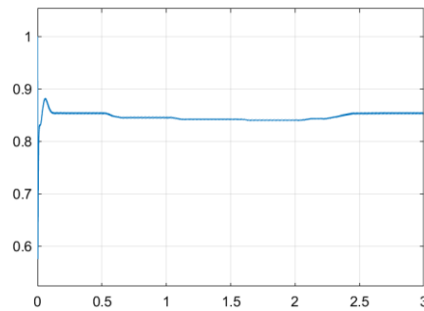


Figure 24 VSC “m” value waveform

IdIq (pu) waveforms display VDC regulator outputs and PLL&Measurements from VSC control. Figure 25 shows the waveform of Idref (orange) and Iq (blue).

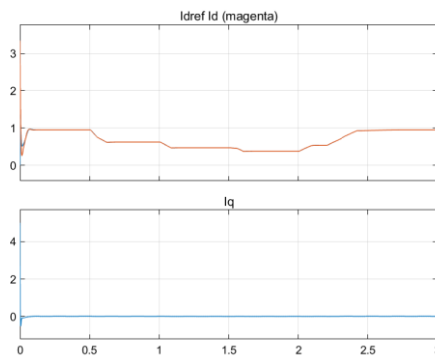


Figure 25 IdIq (pu) waveforms

Next in the system is an RL branch ( $1e-3$  Ohms and  $45e-6$  H) connected to the VSC. Then a capacitor bank with a capacity of 40 kvar is connected to the

system. The converter is coupled to the grid via a 400 kVA 260 V/25 kV three-phase coupling transformer with two windings. The first winding connection (ABC terminals) is Y grounded, and the second winding connection (abc terminals) is Delta (D1). Figure 26 displays the connection topology of the mentioned components.

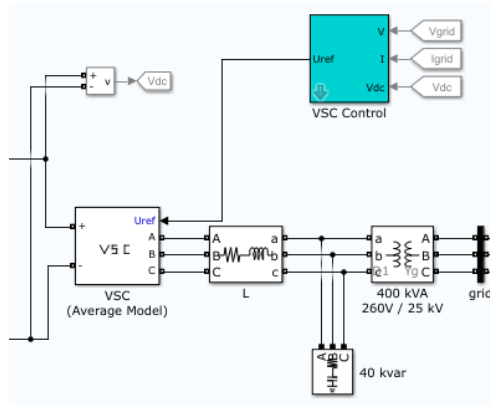


Figure 26 VSC, three-phase transformer and VI measurement connection topology

Parameters of the three-phase transformer block are shown in Figure 27.

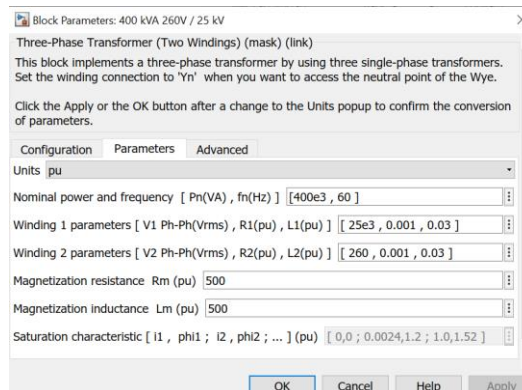


Figure 27 Block parameters of three-phase transformer in MATLAB/Simulink®

The expanded three-phase VI measurement block is shown in Figure 28. Vgrid and Igrid are then used in grid scope to illustrate the waveforms.

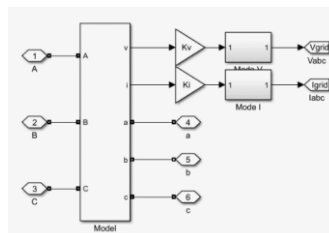


Figure 28 Expanded three-phase VI measurement block

The circuit used to generate the PQ waveform is shown in Figure 29. V I PQ grid scope (Figure 30) displays the V, I and PQ waveforms. I as the output of the grid current model, V as the output of the grid voltage model and PQ as active and reactive load flow are shown graphically in Figure 31.



Figure 29 PQ waveform generator circuit

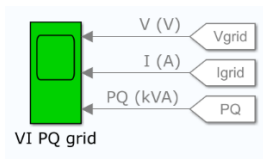


Figure 30 Topology of VI PQ grid scope

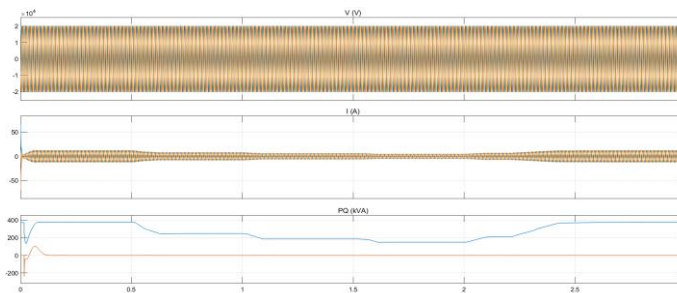


Figure 31 VI PQ waveforms

Table 9 gives the measured values of P and Q regarding to the waveforms.

Table 9 Measured parameters for P and Q (Load profile = 100 kW)

Time (s)	P (kW)	Q (kvar)
0	372	0
0.5	376	0
1	248	0
1.5	187	0
2	150	0
2.5	370	0
3	376	0

A three-phase parallel/series RLC load block is used in the simulation. The configuration of the load block is Y grounded with Constant Z as the load type. The utility grid consists of a three-phase voltage source in series with an RL branch (120 kV/2500 MVA), A 120 kV/25 kV 47 MVA three-phase transformer, grounding transformer, three-phase parallel RLC loads, and three-phase PI section line to model a three-phase transmission line with a single PI section. As a typical North American grid, the grid includes a 25 kV distribution feeder and a 120 kV

equivalent transmission system. Figure 32 displays the connection topology of the mentioned components.

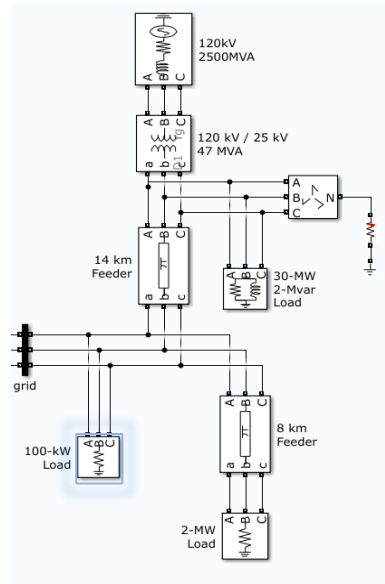


Figure 32 RLC load block and utility grid connection topology

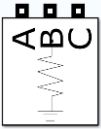
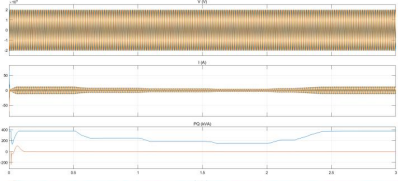
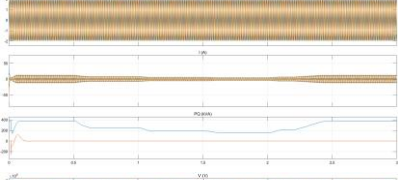
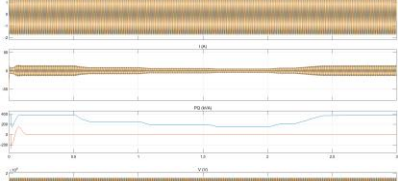
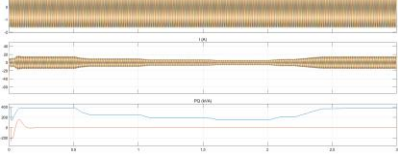
### C. Performance Analysis

In order to analyze the system, we first look at how changes in the load (highlighted load block in Figure 3) may affect the system performance. This study focuses on analyzing the system to find the load limitation or valid performance range. The block figure in MATLAB/Simulink®, load profile, test results, and the V I PQ grid waveforms are all displayed in Tables 10 to 14. The performance analysis process can be divided into performance analysis of active loads and a combination of active and reactive loads in which three-phase series and parallel RLC loads are analyzed. Waveforms and data are gathered for comparison each time a new load profile is evaluated and simulation is carried out.

#### 1. Performance Analysis Under Active Loads

Different resistive loads from 100 kW to 40 MW were tested to analyze the system under active loads. Table 10 demonstrates the test results and the V I PQ grid waveforms. As it is shown in the table, the grid supports the load when the load profile is 30 MW. However, it can be seen through the waveforms that the voltage is decreasing significantly as the load profile is increasing.

Table 10 Performance analysis of various resistive active load profiles

Block Figure	Load Profile	Test Results	V I PQ grid scope
	Active Power P (W): 100 kW	Stable grid/supporting load	
	Active Power P (W): 10 MW	Stable grid/supporting load	
	Active Power P (W): 30 MW	Stable grid/supporting load	
	Active Power P (W): 40 MW	Beginning of non- stability in grid/not supporting load properly	

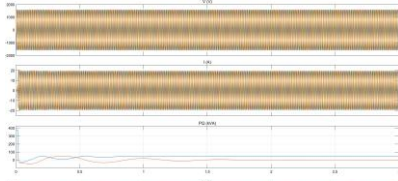
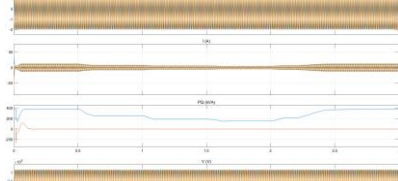
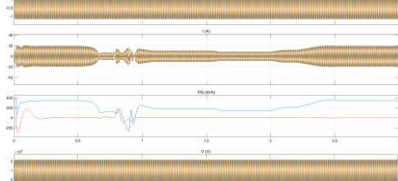
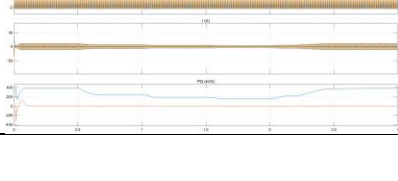
## 2. Performance Analysis Under Active and Reactive Loads

After analyzing the system with a resistive active load, a combination of active and reactive loads is evaluated. We can divide the RLC loads into two groups; series RLC loads and parallel RLC loads. In both groups, resistive loads are considered as the active part, and either capacitive or inductive loads are considered as the reactive part.

### 2.1. Series RLC Load

To analyze the system with a resistive active and capacitive reactive load connected in series form, we commence by changing the load profiles mentioned in Table 11. At first, the grid was not supporting the load, so we decreased the amounts until the waveforms were stable. As test results confirm, the system cannot handle loads with more than an active power of 1 kW and a capacitive reactive power of 1 kvar connected in series.

Table 11 Performance analysis of various resistive active and capacitive reactive load profiles connected in series

Block Figure	Load Profile	Test Results	V I P Q grid scope
	Active Power P (W): 100 kW Capacitive reactive power QC negative var: 40 kvar	Not Stable grid/not supporting load	
	Active Power P (W): 100 kW Capacitive reactive power QC negative var: 1 kvar	Not Stable grid/not supporting load	
	Active Power P (W): 1 kW Capacitive reactive power QC negative var: 100 var	Stable grid/supporting load	
	Active Power P (W): 10 kW Capacitive reactive power QC negative var: 100 var	Not Stable grid/not supporting load	
	Active Power P (W): 1 kW Capacitive reactive power QC negative var: 1 kvar	Stable grid/supporting load	

Next, the resistive active and inductive reactive loads connected in series were analyzed. The test results are listed in Table 12, along with the waveforms. Five different load profiles were examined, and just one of them was acceptable. Loads with lower values of the active power of 1 kW and inductive reactive power of 1 kvar connected in series can be supported.

Table 12 Performance analysis of various resistive active and inductive reactive load profiles connected in series

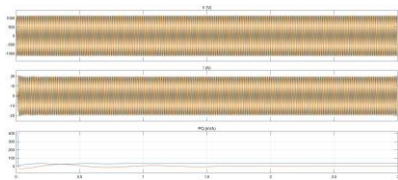
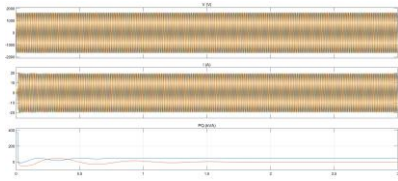
Block Figure	Load Profile	Test Results	V I P Q grid scope
	Active Power P (W): 100 kW Inductive reactive power QL positive var: 100 kvar	Not Stable grid/not supporting load	
	Active Power P (W): 100 kW Inductive reactive power QL positive var: 1 kvar	Not Stable grid/not supporting load	

Table 12 Performance analysis of various resistive active and inductive reactive load profiles connected in series Continue

	Active Power P (W): 1 kW Inductive reactive power QL positive var: 1 kvar	Stable grid/supporting load	
	Active Power P (W): 10 kW Inductive reactive power QL positive var: 1 kvar	Not Stable grid/not supporting load	
	Active Power P (W): 1 kW Inductive reactive power QL positive var: 10 kvar	Not Stable grid/not supporting load	

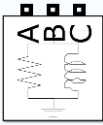
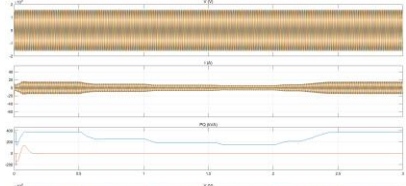
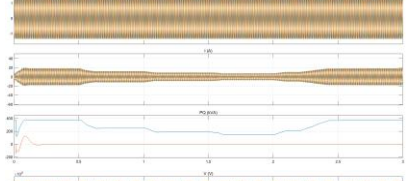
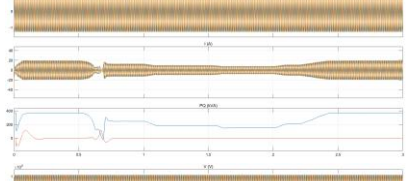
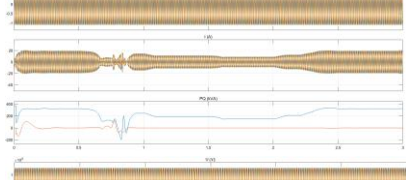
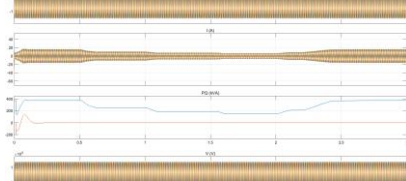
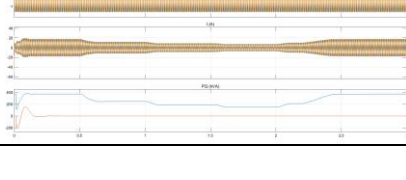
## 2.2. Parallel RLC Load

Table 13 demonstrates performance analysis for loads with resistive active and inductive reactive power values connected in parallel. Ten different load profiles were examined. As shown in the table and the grid waveforms, the system can tolerate loads with less than an active power of 50 MW and inductive reactive power of 15 Mvar.

Table 13 Performance analysis of various resistive active and inductive reactive load profiles connected in parallel

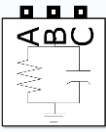
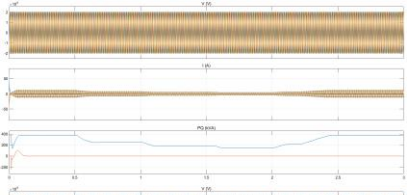
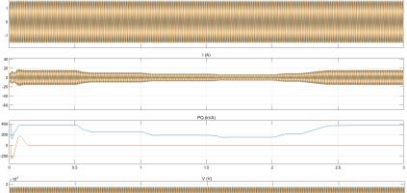
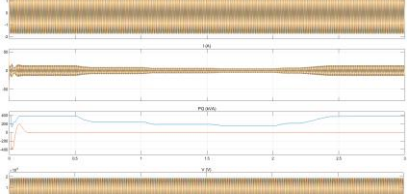
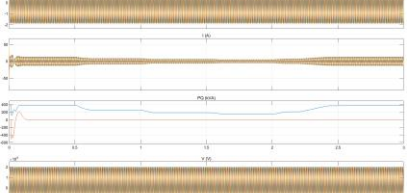
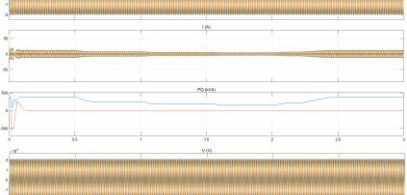
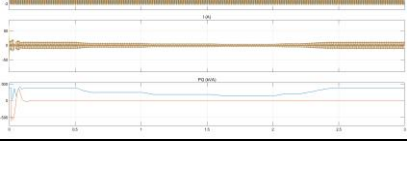
Block Figure	Load Profile	Test Results	V I PQ grid scope
	Active Power P (W): 100 kW Inductive reactive power QL positive var: 10 Mvar	Stable grid/supporting load	
	Active Power P (W): 100 kW Inductive reactive power QL positive var: 100 Mvar	Not Stable grid/not supporting load	
	Active Power P (W): 100 MW Inductive reactive power QL positive var: 10 Mvar	Not Stable grid/not supporting load	
	Active Power P (W): 10 MW Inductive reactive power QL positive var: 10 Mvar	Stable grid/supporting load	

Table 13 Performance analysis of various resistive active and inductive reactive load profiles connected in parallel  
Continue

	Active Power P (W): 30 MW Inductive reactive power QL positive var: 10 Mvar	Stable grid/supporting load	
	Active Power P (W): 30 MW Inductive reactive power QL positive var: 30 Mvar	Stable grid/supporting load	
	Active Power P (W): 30 MW Inductive reactive power QL positive var: 40 Mvar	Not Stable grid/not supporting load	
	Active Power P (W): 50 MW Inductive reactive power QL positive var: 50 Mvar	Not Stable grid/not supporting load	
	Active Power P (W): 30 MW Inductive reactive power QL positive var: 15 Mvar	Stable grid/supporting load	
	Active Power P (W): 50 MW Inductive reactive power QL positive var: 15 Mvar	Stable grid/supporting load	

Six different load profiles were analyzed to study the system performance under loads with active and capacitive reactive power values connected in parallel form. The amounts of the loads were increased during the test to see the system limitation. The system is stable until the load reaches the active power value of 50 MW and capacitive reactive power of 30 Mvar.

Table 14 Performance analysis of various resistive active and capacitive reactive load profiles connected in parallel

Block Figure	Load Profile	Test Results	V I PQ grid scope
	Active Power P (W): 100 kW Capacitive reactive power QC negative var: 100 kvar	Stable grid/supporting load	
	Active Power P (W): 50 MW Capacitive reactive power QC negative var: 100 kvar	Stable grid/supporting load	
	Active Power P (W): 50 MW Capacitive reactive power QC negative var: 20 Mvar	Stable grid/supporting load	
	Active Power P (W): 50 MW Capacitive reactive power QC negative var: 30 Mvar	Stable grid/supporting load	
	Active Power P (W): 50 MW Capacitive reactive power QC negative var: 40 Mvar	Not Stable grid/not supporting load	
	Active Power P (W): 50 MW Capacitive reactive power QC negative var: 50 Mvar	Not Stable grid/not supporting load	

## V. CONCLUSION AND FUTURE WORK

This chapter concentrates on the critical findings obtained by investigating a grid-connected PV system. After analyzing and performing experiments, a valid performance range was achieved for the presented system. Some ideas for future work also have been recognized.

This dissertation intends to observe the system's behavior by analyzing the system's performance under different load conditions. First, the model of the system was simulated in MATLAB/Simulink<sup>®</sup>. To observe how the system operates, each component was analyzed with the help of the software. Parameters were measured, and waveforms were studied to comprehend the connection and effects of changing one parameter on the system. The information and learnings were classified and compared to the research done by the scholars. The input data used in the simulation was not conducted from any datasets since the main idea was to find a valid performance range for the system. The outcomes justify the system limitation or the valid performance range estimated for various load conditions.

The simulation results indicated that the presented grid-connected PV system with 400 kW capacity could afford to support loads up to 30 MW for resistive loads, 50 MW and 15 Mvar for resistive active and inductive reactive loads connected in parallel form, 50 MW and 30 Mvar for resistive active and capacitive reactive loads connected in parallel form, 1 kW and 1 kvar resistive active and capacitive reactive loads connected in series and, 1 kW and 1 kvar resistive active and inductive reactive loads connected in series.

In conclusion, the study shows that the system performs well and can satisfy the load demand in the mentioned range. Based on the ideas presented in this study, a set of future work and new research areas can be suggested; such as:

- Extend the study by correlating the predictive model with actual field data.

- The possibility of implementing the PV system in a location.
- Developing the system through the integration of other renewable energy sources, such as wind turbines.

## VI. REFERENCES

### BOOKS

- SATPATHY, R.K. AND PAMURU, V., 2020. **Solar PV power: design, manufacturing and applications from sand to systems**. Academic Press.
- SUMATHI, S., KUMAR, L.A. and SUREKHA, P., 2015. **Solar PV and wind energy conversion systems: an introduction to theory, modeling with MATLAB/SIMULINK, and the role of soft computing techniques** (Vol. 1). Switzerland: Springer.

### ARTICLES

- HALABI Laith M., MEKHILEF Saad, OLATOMIWA Lanre and HAZELTON James, "Performance analysis of hybrid PV/diesel/battery system using HOMER: A case study Sabah, Malaysia", **Energy Conversion and Management**, Volume 144, 2017, Pages 322-339, ISSN 0196-8904, <https://doi.org/10.1016/j.enconman.2017.04.070>.
- MOSOBI, RINCHIN W., and GAO Sarsing. "Performance Analysis of Hybrid Solar-Wind-Microhydro System in Islanded Mode." In **2018 IEEE Region Ten Symposium (Tensymp)**, pp. 106-111. IEEE, 2018.
- JAVED, & ASHFAQ, HAROON & SINGH, & HUSSAIN, SUHAIL & USTUN, TAHA SELIM. (2019). "Design and Performance Analysis of a Stand-alone PV System with Hybrid Energy Storage for Rural India". **Electronics**. 8. 952. 10.3390/electronics8090952.
- BHAN, V., SHAIKH, S.A., KHAND, Z.H., AHMED, T., KHAN, L.A., CHACHAR, F.A. AND SHAIKH, A.M., 2021. "Performance evaluation of perturb and observe algorithm for MPPT with buck–boost charge controller in photovoltaic systems". **Journal of Control, Automation and Electrical Systems**, 32(6), pp.1652-1662.
- SURENDRA, H.H., SUDHINDRA, K.R., ARCHANA, H.R. and MADHUSUDHAN, K.N., 2022, December. "Performance Analysis of Standalone PV System

- using System Advisor Model-A Case Study”. In **2022 IEEE International Conference on Current Development in Engineering and Technology (CCET)** (pp. 1-4). IEEE.
- SHAKIR, A.M., YOUSIF, S.M. AND MAHMOOD, A.L., 2022. “An optimum location of on-grid bifacial based photovoltaic system in Iraq”. **International Journal of Electrical & Computer Engineering** (2088-8708), 12(1).
- CHABACHI, S., NECAIBIA, A., ABDELKHALEK, O. et al. “Performance analysis of an experimental and simulated grid connected photovoltaic system in southwest Algeria”. **Int J Energy Environ Eng** 13, 831–851 (2022). <https://doi.org/10.1007/s40095-022-00474-9>
- REHMAN, S., NATARAJAN, N., VASUDEVAN, M., MOHAMMED, A.B., MOHANDÉS, M.A., KHAN, F. and AL-SULAIMAN, F.A., 2022. “Performance evaluation of grid-connected photovoltaic system for Kuttiaady village in Kerala, India”. **Environmental Science and Pollution Research**, pp.1-13.
- DESHMUKH, A. N., & CHANDRAKAR, V. K. (2022). “Design and Performance Analysis of Grid-Connected Solar Photovoltaic System with Performance Forecasting Approach (PFA)”. **Journal of The Institution of Engineers (India): Series B**, 103(5), 1521-1532.
- AMIR, M., PRAJAPATI, A.K. and REFAAT, S.S., 2022. “Dynamic performance evaluation of grid-connected hybrid renewable energy-based power generation for stability and power quality enhancement in smart grid”. **Frontiers in Energy Research**, 10, p.222.
- NARASIMMAN, K., GOPALAN, V., BAKTHAVATSALAM, A.K., ELUMALAI, P.V., SHAJAHAN, M.I. and MICHAEL, J.J., 2023. “Modelling and real time performance evaluation of a 5 MW grid-connected solar photovoltaic plant using different artificial neural networks”. **Energy Conversion and Management**, 279, p.116767.
- MADETI, S.R. and SINGH, S.N., 2017. “Monitoring system for photovoltaic plants: A review”. **Renewable and Sustainable Energy Reviews**, 67, pp.1180-1207.
- ASSADEG, J., SOPIAN, K. and FUDHOLI, A., 2019. “Performance of grid-connected solar photovoltaic power plants in the Middle East and North Africa”.

**International Journal of Electrical and Computer Engineering**, 9(5), p.3375.

HASANEEN, B.M. AND MOHAMMED, A.A.E., 2008, March. "Design and simulation of DC/DC boost converter". In **2008 12th International Middle-East Power System Conference** (pp. 335-340). IEEE.

ELMELEGI, A. and AHMED, E.M., 2015, December. "Study of Different PV Systems Configurations Case Study: Aswan Utility Company". In **17th International Middle East Power Systems Conference**, Mansoura University, Egypt.

SRITA, S., SOMKUN, S., KAEWCHUM, T., RAKWICHIAN, W., ZACHARIAS, P., KAMNARN, U., THONGPRON, J., AMORNDECHAPHON, D. AND PHATTANASAK, M., 2022. "Modeling, simulation and development of grid-connected voltage source converter with selective harmonic mitigation: Hil and experimental validations". **Energies**, 15(7), p.2535.

KALHARI MADHUSHIKA; BANDARA HASITHA ERANDA; EDIRIWEERA SAMPATH (2022), "Power Factor Improvement of Industrial Loads using a Capacitor Bank and a Solar PV System", **7th International Conference on Advances in Technology and Computing (ICATC 2022)**, Faculty of Computing and Technology, University of Kelaniya Sri Lanka. Page 6-11.

BELOV, S.I., TSEDYAKOV, A.A. and GALKIN, M.M., 2022, June. "Simulation modeling of a two-winding three-phase voltage transformer in the MATLAB program". In **IOP Conference Series: Earth and Environmental Science** (Vol. 1045, No. 1, p. 012072). IOP Publishing.

#### **ELECTRONIC SOURCES**

MATHWORKS, Inc. 400-kW Grid-Connected PV Farm  
<https://www.mathworks.com/help/sps/ug/400-kw-grid-connected-pv-farm-average-model.html>

#### **OTHER SOURCES**

IRENA (2023), Renewable capacity statistics 2023, International Renewable Energy Agency, Abu Dhabi.

IEA snapshot of global PV market 2022 IEA PVPS Task 1 Strategic PV Analysis and  
Outreach Report IEA-PVPS T1-42:2022 April 2022 ISBN 978-3-  
907281-31-4

IEA snapshot of global PV market 2023 IEA PVPS Task 1 Strategic PV Analysis and  
Outreach Report IEA-PVPS T1-44:2023 April 2023 ISBN 978-3-907281-  
43

